Anthropogenic heat release in an old European agglomeration (Toulouse, France)

G. Pigeon,[a]* D. Legain,[a] P. Durand[b] and V. Masson[a]

[a] *Centre National de Recherches Météorologiques, Météo-France/CNRS-GAME, 42 av. Coriolis, 31057 Toulouse Cedex, France*
[b] *Laboratoire d'Aérologie, UMR 5560 CNRS - Université Paul Sabatier Toulouse III, Toulouse, France*

Abstract:

The anthropogenic heat release, Q_F, has been estimated for the old European agglomeration of Toulouse (France) from February 2004 to March 2005 in the frame of the CAPITOUL experiment. Surface energy balance (SEB) measurements have been conducted at a downtown site, over a dense urban area. A method is proposed to estimate Q_F at the local scale around this site from observations, as the daily residual term of the SEB equation. The values obtained from this method are in agreement with what can be expected: Q_F estimates are around 70 W m^{-2} during winter and 15 W m^{-2} during summer. On a larger scale (that of the agglomeration), an energy consumption inventory was conducted for the period of the field campaign with a 1-day temporal resolution and a 100-m spatial resolution. The estimates of Q_F obtained with this second method were analysed at the local scale around the measurements site, and compared with estimates computed from the energy budget observations. For the winter period, both estimates are in good agreement. For the summer period, the method based on SEB measurements seems to underestimate Q_F which is estimated around 30 W m^{-2} from the inventory. The simultaneous estimate of Q_F, with these two independent methods is a strength of this study.

At the scale of the agglomeration, the basal state of energy consumption (observed during the summer period) varies between 25 W m^{-2} for the densest areas to less than 5 W m^{-2} for the residential suburban areas. In the regions crossed by the major roads, the traffic is the major source during summer. Then during the winter period, Q_F can reach 100 W m^{-2} in the densest areas of Toulouse whereas it ranges between 5 and 25 W m^{-2} in the suburban areas. Copyright © 2007 Royal Meteorological Society

KEY WORDS   urban climate; urban energy balance; anthropogenic heat source; energy consumption inventory; CAPITOUL

Received 29 September 2006; Revised 26 February 2007; Accepted 26 February 2007

INTRODUCTION

In comparison to the other surfaces of the earth, urban areas are subject to an additional source of energy: the anthropogenic heat release, noted Q_F (Oke, 1987). The flux Q_F results mainly from the consumption of energy by human activity: heating of buildings, traffic, electrical appliances, industry, and air conditioning. The anthropogenic heat has been identified by Oke (1982) to contribute to the urban climate modification at the canopy scale, the local scale (neighbourhood) and the mesoscale (agglomeration scale). It has been shown that taking it into account in atmospheric numerical simulations could result in a temperature increase by a few degrees in certain conditions (Kimura and Takahashi, 1991; Ichinose *et al.*, 1999; Kikegawa *et al.*, 2006), or even a modification of the wind field (Khan and Simpson, 2001).

In the former studies, two methods have been developed to estimate Q_F but they have never been compared on the same spatial and temporal scale. The first method is based on inventories of energy consumption and has been applied by Grimmond (1992) for a suburban area of Vancouver (Canada), by Kłysik (1995) for the city of Łódź (Poland), by Ichinose *et al.* (1999) for Tokyo (Japan) and by Sailor and Lu (2004) for different cities in the United States. The estimation of Q_F with a high spatial and temporal resolution by this method is almost impossible considering the wide range of energy uses and the organization of energy distribution. Most of the time, this method is based on energy consumption budget at the scale of a city, or even at wider scales, and at a monthly time resolution. However, other sources of information, such as the patterns of population density, can be used to estimate the spatio-temporal variability at smaller scales (Sailor and Lu, 2004). The second method is based on surface energy balance (SEB) measurements (Offerle *et al.*, 2005). The advantage of this method is that it makes it possible to estimate Q_F with an hourly time resolution, but its weakness is that it is limited to the local scale (typically a neighbourhood or a few hundreds meters) around the measurement site.

The objective of this study is to estimate *simultaneously* Q_F with these two methods for the agglomeration

* Correspondence to: G. Pigeon, Centre National de Recherches Météorologiques, Météo-France/CNRS-GAME, 42 av. Coriolis, 31057 Toulouse Cedex, France. E-mail: gregoire.pigeon@meteo.fr

of Toulouse located in the south–west of France. From February 2004 to March 2005, the CAPITOUL [Canopy and Particles Interactions in Toulouse Urban Layer (Masson *et al.*, 2004)] field campaign was conducted over the agglomeration to monitor, during a full year, the SEB, the urban heat island and the urban boundary layer structure. A method, simpler than the one developed by Offerle *et al.* (2005), is presented to estimate Q_F from SEB measurements made in the downtown area of Toulouse. Also, an inventory of energy consumption is conducted at the agglomeration scale with a 1-day time resolution and a 100-m horizontal resolution. Given the high spatial resolution of the inventory of energy consumption, it can be compared with the estimates from the measurements at the downtown site. Finally, the spatio-temporal variability of Q_F at the agglomeration scale is analysed with a modelling perspective.

DESCRIPTION OF THE SITE

Toulouse agglomeration

Toulouse ($1°26'4''$E, $43°36'15''$N) is located in the south–west of France, 80 km to the north of the Pyrenees chain, 140 km to the west of the Mediterranean Sea and 220 km to the east of the Atlantic Ocean. The agglomeration is at the intersection of oceanic and Mediterranean influences and subject to a mild temperate climate from fall to spring and to dry, hot summers. The mean annual precipitation is 656 mm and the sunshine duration is 2047 h (from data collected during the 1961–1991 period at the Toulouse-Blagnac meteorological station). Table I gives the mean monthly temperature during the field campaign from February 2004 to February 2005. Given the climate of the city, the domestic heating period in Toulouse extends approximately from the end of October to the mid of May, which corresponds to the period during which the mean daily temperature is lower than 15 °C.

The area covered by the district of Toulouse is quite circular (Figure 1) with a diameter of 7 km and a population of 426 700 inhabitants (in 2004), whereas the whole agglomeration extends over 20 km with a population estimated to be between 1 065 000 and 1 080 000 inhabitants (data from the National Institute for Statistics and Economic Studies for 2004). The area considered in this study and referred as the agglomeration is the total area presented in Figure 1. Following Oke (2006)

recommendations, we propose to describe the geography of the city with the Wanner and Filliger (1989) classification: the effects of urbanization variability dominate the topographic influence; the Garonne river crosses the agglomeration in its middle and the site is classified as 'Valley within urban area'.

Measurements site and data processing

A SEB measurements site was located in the dense old core of Toulouse. The site location can be seen on Figure 1 and the aerial photography presented in Figure 2, and its characteristics have been gathered in Table II.

The micro-meteorological instrumentation (Table III) was mounted on the head of a telescopic tower set up on a terrace roof. The building has typical dimensions in comparison to those of the surrounding and its roof is at 20 m above the street. When the wind speed at the top of the tower was lower than 17 m s^{-1},
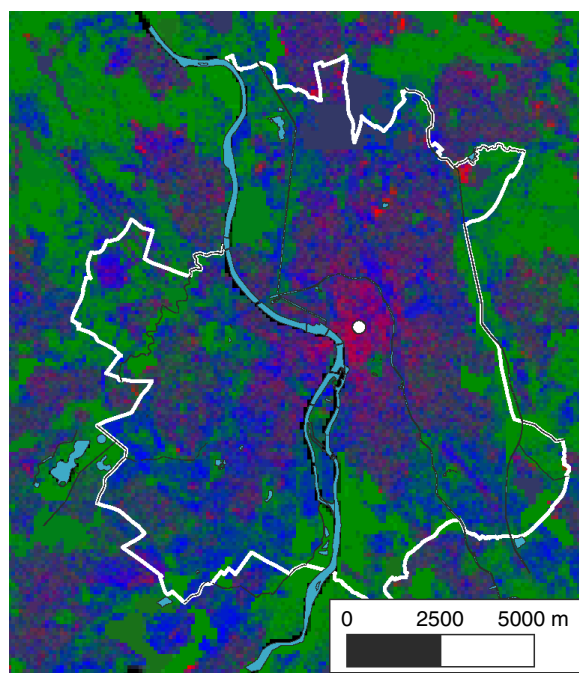

Figure 1. Colour composite of building plan area density (pad, in red), vegetation pad (in green) and road pad (in blue) with 100-m resolution over the agglomeration of Toulouse. The white line represents the limit of Toulouse district. This figure is available in colour online at www.interscience.wiley.com/ijoc

Table I. Monthly climate parameters during the field campaign at Toulouse-Blagnac meteorological station (WMO ID 76390). T_{min} and T_{max} are the minimum and maximum daily averages, respectively.

Year	2004											2005	
Month	F	M	A	M	J	J	A	S	O	N	D	J	F
T_{mean} (°C)	6.3	8.6	11.3	15.4	21.3	22.2	22.7	20.3	16.7	7.4	6.4	5.3	4.2
T_{min} (°C)	1.7	4.1	7.3	10.3	15.7	16.6	17.3	14.8	12.7	4.1	3.5	1.9	0.9
T_{max} (°C)	10.9	13.2	15.4	20.5	26.9	27.8	28.0	25.8	20.7	10.8	9.3	8.8	7.5
Precipitations (mm)	10.2	63.8	105.2	73.6	19.6	33.0	59.8	25.4	161.8	29.2	39.2	21.4	20.2

Table II. Characteristics of the measurement site.

Parameter	Value
Building plan area density (pad)	0.54
Road pad	0.38
Vegetation pad	0.08
Wall surface density[a]	1.3
Canyon aspect ratio	1.4
Mean building height (m)	15
Oke (2004) urban climate zone	2

[a] Ratio between wall surface and total horizontal surface.

Figure 2. Aerial photography around the measurement site (marked with a black disk). The black circle indicates the 500-m distance around the tower. This figure is available in colour online at www.interscience.wiley.com/ijc

the measurement level was at 27.5 m above the roof. When the wind speed was between 17 and 25 m s^{-1}, the instrumentation was set at 18.5 m above the roof. For stronger winds and stormy weather, the instruments were lowered down to the roof level. The measurements recorded in the latter conditions are not used in this study. The sensible and latent heat fluxes were computed using eddy-covariance technique, on half-hourly periods. Wind components were first corrected with two successive rotations (azimuth and pitch corrections). Then, before

computing the covariance, the time series were high-pass filtered with a recursive filter according to McMillen (1988), with the filter parameter set to 200 s. The mean daily estimates of Q_F (see next section) have been computed for days when the tower was in the intermediate or upper position. Missing data have been interpolated linearly when less than two consecutive data were missing.

METHODS

Estimates of Q_F from energy balance measurements

The SEB framework developed by Oke (1988) for urban areas applies to a control volume extending from the ground to the top of the urban canopy layer:

$$Q^* + Q_F = Q_H + Q_E + \Delta Q_S + \Delta Q_A \qquad (1)$$

where Q^* is the net radiation at the top of the volume, Q_F gathers the anthropogenic heat releases as mentioned previously, Q_H is the sensible heat flux, Q_E is the latent heat flux, ΔQ_A is the heat (or equivalent latent heat) advection through the sides of the control volume and ΔQ_S is the storage of heat by the elements of the control volume. Q_F is always positive, whereas Q^* (resp. Q_H and Q_E) is positive downward (resp. upward). ΔQ_S and ΔQ_A are positive when they correspond to a gain of heat for the volume. In this study, as in most of field measurement over urban areas, only three terms of the SEB equation (Q^*, Q_H and Q_E) are measured with micro-meteorological techniques. The residual R of these terms is thus expressed as:

$$R = Q^* - (Q_H + Q_E) \qquad (2)$$

From Equation (1), the residual is also expressed by:

$$R = \Delta Q_S + \Delta Q_A - Q_F \qquad (3)$$

Several estimates of ΔQ_A have been presented recently (Lee and Hu, 2002; Spronken-Smith *et al.*, 2005; Pigeon *et al.*, 2007). Pigeon *et al.* (2007) showed that advection is considerable in the case of strong temperature or moisture gradients associated with the sea-breeze flow over a

Table III. Instrumentation of the tower in the dense old core of Toulouse.

Instrument/Model	Manu-facturer	Sampling frequency (Hz)	Precision
3D sonic anemometer/thermometer, Horizontal HS1199 (SN 00401)	Gill	50	wind <1% rms sound speed <0.5%
Infra-red hygrometer and CO_2 analyser, Licor 7500 (SN PG326B)	Licor	20	H_2O 3%
Net radiometer, CNR1 (SN 03700)	Kipp & Zonen	0.1	10% in daily average
Thermo-hygrometer HMP233 (SN S3830005)	Vaisala	0.1	T 0.2 °C RH 3%
Barometer, PTB220 class A	Vaisala	0.1	0.2 hPa

coastal city. From the measurements performed during CAPITOUL around the study site, Pigeon *et al.* (2004) have shown that the temperature and moisture horizontal gradients are weak at the local scale, and ΔQ_A is therefore neglected in the present study. ΔQ_S has received much attention in the literature (Oke and Cleugh, 1987; Grimmond *et al.*, 1991; Arnfield and Grimmond, 1998; Grimmond and Oke, 1999; Offerle *et al.*, 2005; Weber, 2005). On time scales of a few hours, ΔQ_S is a strong component of the SEB (58% of daytime Q^* for Mexico City in Oke *et al.*, 1999). It is considered to be the largest of the non-measured terms (Q_F, ΔQ_S and ΔQ_A), and is often approximated by R (Oke and Cleugh, 1987). The basic assumption is that ΔQ_S should vanish over longer timescales (one day or multiple of entire days), otherwise it would lead to unrealistic temperature changes of the urban fabric (Christen and Vogt, 2004). Results supporting this hypothesis are presented by Offerle *et al.* (2005). They present an original method to get hourly values of ΔQ_S, at the local scale, by combining numerical simulation and measurements. Their conclusion is that for a site with characteristics similar to those of Łódź and for monthly periods, $|\Delta Q_S|$ is on average lower than 10 W m^{-2}, and that, for such periods, the residual term R could be used to estimate Q_F with an accuracy of 10 W m^{-2}. Toulouse site is slightly denser than Łódź (impervious pad of 0.92 for Toulouse vs 0.70 for Łódź), however, because of its oceanic climate, the temperature changes are smoother than in Łódź, which is submitted to a continental climate. The daily heat storage, therefore, should be weaker. Moreover, Q_F values estimated from the inventory (Section 'Results and Discussion') at the local scale around our measurement site are larger than the $\overline{\Delta Q_S}$ estimates presented by Offerle *et al.* (2005), even in summer conditions. Hence, we assume that the average of the residual over a 1-day (or multiples of 1-day) period can be used to estimate Q_F with the following relation:

$$\overline{\Delta Q_S} \ll \overline{Q_F} \text{ and } \overline{Q_F} = -\overline{R} \qquad (4)$$

where the overbar denotes the average over a period of *n*-day. This assumption has been used on a one-year time scale by Christen and Vogt (2004) when they found a missing energy source in their energy budget.

A potential problem in evaluating Q_F as the mean of the residual is that this estimate suffers from the accumulation of the errors on the three measured terms of the SEB. A review about this issue can be found in Foken (2006). According to Kohsiek *et al.* (in press), the accuracy of the CNR1 net radiometer from Kipp & Zonen can be estimated between 5 to 20%. Concerning Q_H and Q_E, the results of Mauder *et al.* (in press) on a set of sensors give accuracies of the order of 10% and 15%, respectively. If we assume that all these errors are systematic and act in the same way (which rarely occurs), the resulting error on Q_F could reach 20 to 40% of Q^*. On the hand, the non-closure of the energy balance estimated with the eddy-covariance method is

well known in the micro-meteorological community (Wilson *et al.*, 2002; Foken, 2006) and would result in an underestimation of Q_F with this method. Foken (2006) proposes a range between 0–30% for this error. Finally, in a mid-latitude city like Toulouse, Q_F is larger in winter than in summer, so the relative accuracy increases in winter. All these considerations should be kept in mind when considering the following results.

Estimates of Q_F from the inventory of energy consumption

Estimating Q_F from the inventory of energy consumption is a classical approach (Grimmond, 1992; Kłysik, 1995; Ichinose *et al.*, 1999; Sailor and Lu, 2004). This method assume that the final stage of all energy use is heat and that the delay between energy use and its restitution to heat is zero (Sailor and Lu, 2004). In this study, the inventory of energy consumption has been constructed at two different spatial scales: the local scale around the downtown measurement site and the agglomeration scale. At the local scale, an inventory was proposed on a circular, 500 m radius area around the micro-meteorological tower because such an area can be considered representative of the footprint of the measurements performed on the tower (Lemonsu *et al.*, 2004). Q_F computed from this inventory at the local scale has been compared with the values computed from micro-meteorological measurements as described above. At the scale of the whole agglomeration, the inventory was intended to assess the spatial variation of Q_F. In the future, it will be used to constrain the urban surface scheme in numerical simulations, or to evaluate the performance of such schemes if they are able to compute all the terms of the city energy budget. In this inventory, we have estimated separately the different sources that contribute to Q_F: releases from traffic (Q_{FT}) and consumption of electricity and gas from fixed locations (Q_{FB}). These fixed sources include housings, tertiary economy sector and industries. Toulouse is not a very industrialised place and most of industries (Airbus company, for example) are outside the domain of this study. For small industries inside the domain, their use of electricity and gas were included in the available consumption data set. Though there were some uncertainties in the location of the latter sources, they should not affect the results significantly, because these sources were quite scarce and cover small areas. For domestic housings, 90% of energy uses are electricity or gas. We have assumed that this value is also valid for tertiary sector buildings. According to previous studies (Grimmond, 1992; Sailor and Lu, 2004), we have neglected the input from human metabolism. The rasterization of the inventory has been carried out using a Geographical Information System (GIS).

The spatial and temporal variability of Q_F has been carried out separately. This methodology is supported, first, by the fact that the locations of infrastructures (roads, buildings) where energy is consumed do not evolve much at the considered time scale, and, second,

by the major influence of seasonal and human activity cycles on the temporal evolution of Q_F.

Rasterization of traffic releases

For a domain of surface A, the energy flux released by traffic at a time t can be computed as:

$$Q_{FT}(t) = (1/A) \times \sum_i n_{vi}(t) \times l_i \times EV \qquad (5)$$

where suffix i indicates the different traffic sections inside A, $n_{vi}(t)$ is the number of vehicles travelling on section i at time t expressed in s^{-1}, l_i is the length of section I and EV is the mean energy used per vehicle and per length unity. EV is expressed in $J\,m^{-1}$ and depends on the fleet distribution of vehicles, the fuel economy of each class of vehicles and the heat of combustion of the different fuels. In France, two fuels are used: gasoline for which the heat of combustion is 43.8 MJ kg^{-1} and diesel for which the heat of combustion is 42.5 MJ kg^{-1} (Guibet, 1997). The combustion of fuels also produces water vapour that is sensed by the micrometeorological system and taken into account in the measurements of Q_E. This contribution should theoretically not be included in the SEB (except if this water vapour condensate) but it cannot be separated from the water vapour flux due to evaporation at the surface. It has, therefore, been taken into account in order to be consistent with the estimates issued from measurements. Both fuels can be modelled by octane and, for this hydrocarbon, the heat corresponding to the change of state of the water vapour rejected by its combustion is 8% of the heat of combustion (Guibet, 1997). As a result, the latent heat flux resulting from traffic represents 8% of the estimates of heat release. The fleet distribution and the fuel economy have been taken from Hugrel and Joumard (2004, 2006). Corresponding figures are summarised in Table IV. The resulting EV is 4710 J m^{-1}, which is 18% higher than the value used by Sailor and Lu (2004).

The length of each section as well as the Mean Annual Number of Vehicles travelling per Day (MANVD) on it were available from the GIS of the Transportation Office of Toulouse district administration (Service circulation-transports, Mairie de Toulouse), the Traffic Office of the Equipment Direction of Haute-Garonne administrative region (Cellule d'Exploitation et d'Ingénierie du Trafic, Direction Départementale de l'Equipement

de la Haute-Garonne, DDE31-CEIT) and the document 'Journey Observatory – Journey global management system of Toulouse agglomeration' (Observatoire des déplacements – Système de Gestion Globale des Déplacement de l'Agglomération Toulousaine) edited by the town planning Agency (Agence d'Urbanisme et d'Aménagement du Territoire).

To compute the spatial variation of Q_{FT} in the agglomeration, the traffic database has been analysed in a GIS on a 100-m resolution grid. For each cell, we used Equation (5) to compute the mean annual value of Q_{FT}. At the local scale around the measurement site, we have extracted the data concerning the sections inside the 500-m area around the tower location (18.5 km of roads in total). For the major sections (5.2 km), the traffic is regularly assessed (every 5 years) and the MANVDs are collected in a GIS. For the other sections, a MANVD of 2000 vehicles per day has been chosen (personal communication from the Toulouse Transportation office). Moreover, inside this area, two permanent counters permanently record the traffic on an hourly basis. To take advantage of this information and to produce a more precise estimate of traffic during the field campaign on an hourly basis, we have weighted this time series by the ratio of the MANDV of each section to the MANDV of the two hourly sampled sections. The days with missing data have been completed with mean daily cycle of the corresponding day type (weekday, Saturday and Sunday).

Rasterization of electricity and gas releases

The electricity and gas consumption have been rasterized using the same method. Three levels of information have been used to produce a high spatial resolution (100 m) map of energy uses with a good temporal resolution.

Real energy delivery. The real deliveries of electricity and gas have been provided for the entire period covered by the field campaign. The electric network is separated in 14 districts and, for each, the 10 min mean power load time series has been provided. For gas, the time series of delivery was representative of the whole urban area and was available at a daily sampling rate. The latent heat release associated with the combustion of gas has been taken into account (see previous section for justification) and it represents 10% of the total energy.

Statistical energy uses. The domestic uses of energy are regularly analysed by the French administration. The mean annual consumptions of energy have been provided by the regional observatory of energy (Observatoire Régional de l'Energie en Midi-Pyrénées – OREMIP) according to the type of housing (collective or individual building), the kind of energy (electricity, gas, wood...) and the function for which this energy is used (heating, hot water, cooking, electrical appliances). The corresponding values are presented in Tables V and VI. Then, the spatial distribution of housing over irregular districts, sorted according to the mean energy consumptions presented in Table V, were purchased to INSEE (National

Table IV. Fraction of distance covered by, and heat release of the main urban vehicles.

	Fraction of total distance	Heat release (J m^{-1})
Car	0.78	3902
Van	0.13	4911
Heavy vehicles	0.06	16 048
Motorcycle	0.03	1220

Table V. Mean annual energy consumption per domestic housing for building and water heating.

System	Energy	Collective housing		Individual housing	
		Heating (MJ)	Hot water (MJ)	Heating (MJ)	Hot water (MJ)
Collective central heating	Urban network	59299.2	14198.4	–	–
	Gas (network)	50040.0	10800.0	–	–
	Domestic fuel	45100.8	15003.6	–	–
	Electricity	47570.4	4284.0	–	–
	Gas (tank)	50040.0	3340.8	–	–
	Wood, coal	47570.4	15451.2	–	–
Individual heating	Gas (network)	38160.0	6480.0	68040.0	10440.0
	Domestic fuel	57628.8	15033.6	68486.4	15033.6
	Electricity	21024.0	4284.0	36720.0	5436.0
	Gas (tank)	32572.8	7516.8	35913.6	13363.2
	Wood, coal	50112.0	12902.4	60134.4	17416.8
Others	Others	43344.0	4284.0	51001.2	5436.0

Table VI. Mean annual energy consumption per domestic housing for electrical appliances and cooking.

Appliance, equipment	Collective housing		Individual housing	
	Gas (MJ)	Electricity (MJ)	Gas (MJ)	Electricity (MJ)
Cooking: gas only	3960.0	–	5400.0	–
Cooking: mixed	2505.6	1620.0	2923.2	2592.0
Electrical appliances	–	6876.0	–	7968.0

Institute for Statistics and Economic Studies). Combining these two pieces of information, the map of the mean annual domestic energy use has been computed for each kind of energy. At this level of spatial analysis, the resolution of the map was not regular and depended on the INSEE districts map. The real time series of electricity and gas consumption (presented in the previous section) have been distributed over these districts weighted by the ratio of the district mean annual consumption to the mean annual consumption on the whole domain. The location of tertiary activities inside the domain was not available and, considering the structure of Toulouse, a regular distribution over the districts was assumed.

Building spatial distribution. Since the districts described in previous sections are determined from demographic and administrative considerations, they can cover various areas within which the spatial distribution of buildings is often heterogeneous. At this stage of spatial analysis, Q_F was homogeneously distributed inside each district, even for residential districts, which can be very inhomogeneous (e.g. dense housing estates on one side and large parks on the other side of the district). For this kind of districts, knowledge of the spatial distribution of buildings would improve the accuracy of the energy consumption localization. To do so, a raster map of building plan area density (pad) with a 100-m resolution has been built over the agglomeration (Massera, 2005). This high-resolution map has been intersected with the districts map and, for each district, its energy consumption

has been distributed at a 100-m resolution grid according to the distribution of building pad inside it.

Rasterization of other domestic energy uses

Other kinds of energy (urban network, domestic fuel, wood, coal) than electricity or gas are used in Toulouse but their contribution is less than 10%. For these kinds of energy, consumption and delivery are not simultaneous like for electricity or gas. It is impossible, therefore, to estimate real-time consumption with a 1-day sampling rate. Consequently, we rasterized these energy uses with a 100-m resolution using the statistical uses (Table V), the housing distribution, and the pad raster map.

Temporal evolution of Q_F.

Three scales can be considered in the time evolution of Q_F. The annual time scale is dominated by the seasonal cycle, which largely determines Q_{FB} but not Q_{FT}. The working-periods/vacations cycle also impacts the annual evolution of Q_F, but its contribution is certainly weak and difficult to assess since it is partially correlated with the seasonal evolution. The two other time scales to consider are the week and the day. Over these timescales, changes are dominated by variations of human activities. From a climate modelling perspective, it is necessary to separate these cycles according to their controlling factors. In a model like TEB (Masson, 2000), which computes the energy budget of the urban surface, the evolution of Q_{FB} related to the weather conditions is physically resolved while the evolution related to human

activities must be prescribed. Our objective has been to evaluate, for each source of energy for which we had at least the 1-day temporal evolution (traffic, electricity, gas), if the weekly or daily cycles were significant in their temporal evolution.

RESULTS AND DISCUSSION

Q_F at the local scale around the measurements site

Measurements. The mean daily estimates of Q_F from the SEB measurements (as described in Section 'Estimates of Q_F from energy balance measurements') have been compared to the daily mean temperatures T_d (Figure 3). The behaviour of the signal is very consistent with what we can presume for Q_F in a temperate climate: as the temperature decreases, the anthropogenic heat increases. Above a critical temperature T_C, the Q_F estimate appears to be independent of temperature. To estimate T_C, we computed the correlation between Q_F and T_d on a varying range of T_d and we defined T_C as the threshold above which the correlation starts to decrease significantly. A value of $15\,°C$ has been found and corresponds well to the threshold we observe for the heating period. For temperatures lower than T_C, a linear model has been computed (with a determination coefficient $R^2 = 0.83$) and the following relation has been established between Q_F and T_d:

$$Q_F(T_d) = 6.8(T_C - T_d) + 12 \text{ for } T_d \leq T_C \quad (6)$$

with Q_F expressed in $W\,m^{-2}$. In this model, an intercept value of $12\,W\,m^{-2}$ has been found and should correspond to the basal level of Q_F in the absence of heating demand. It compares quite well to the mean value of Q_F for temperatures higher than T_C which is $16\,W\,m^{-2}$. In such conditions, Figure 3 reveals some negative, unrealistic values of Q_F. The influence of ΔQ_S, neglected in our

method, cannot be invoked as the main reason for these wrong estimates because significant daily ΔQ_S would lead to unrealistic temperature changes of the canopy elements. The possible underestimation of sensible or latent heat flux by the eddy-covariance technique becomes acute during summer (because the available energy Q^* is high) and certainly contributes more significantly to this problem.

The local scale inventory of energy consumption. The mean daily release of energy in the 500-m area around the measurements site is presented in Figure 4. The traffic-related release (intermediate grey solid line) is quite constant during the year with a value around $9\,W\,m^{-2}$. The electricity consumption is the dominant term of Q_F over this area. It presents a weak annual variation with values of the order of $30\,W\,m^{-2}$ for the winter and $20\,W\,m^{-2}$ for summer period. Gas consumption (dashed grey line) presents a marked annual cycle: during summer, this consumption is lower than $5\,W\,m^{-2}$ whereas it reaches $30\,W\,m^{-2}$ during winter. The difference in electricity and gas consumption indicates that the temporal variation of an energy source that is mainly used for heating (as is the case for the gas) must be interpreted in a different way from that of electricity that has a wider range of applications. In this downtown area of Toulouse, the housing and energy map indicates that no other kind of energy is used. The total Q_F for this dense urban area of Toulouse (solid black line) varies between 60 and $90\,W\,m^{-2}$ for the winter period and is around $30\,W\,m^{-2}$ for summer. These values are slightly higher than what has been found in other studies. But direct comparisons are quite difficult: Offerle *et al.* (2005), for example, also estimate Q_F at the local scale but their site has a lower building pad and height. The volume to be heated is, therefore, reduced in comparison to our site. They computed Q_F values around $50\,W\,m^{-2}$ in winter and $10\,W\,m^{-2}$ during summer.

Comparison between estimates. The estimates of Q_F from both methods have been averaged on monthly periods (Figure 5). They have roughly the same tendency and magnitude. The first striking difference concerns the warmest months (May, June, and July), when the problem of surface energy imbalance is the largest (Wilson *et al.*, 2002). During the winter period, estimates from micro-meteorological measurements are slightly higher but the difference is smaller than the error of this method (Offerle *et al.*, 2005). On the other hand, estimates computed from micro-meteorological measurements are certainly more complete since they are not limited to gas, electricity, traffic and other sources of energy used for heating. Any additional source of energy that would be difficult to inventory is taken into account, like, for example, the case of commercial buildings that are equipped with generating sets for periods of high energy demand.

Q_F at the agglomeration scale

Basal level of Q_F. Figure 6 represents Q_F over the agglomeration averaged during June, July and August
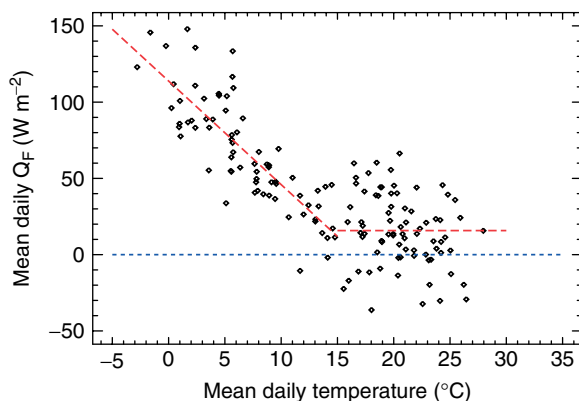

Figure 3. Evolution of mean daily Q_F estimate in function of mean daily air temperature measured at the top of the tower. The short dashed line is the zero anthropogenic heat release. The long dashes line represents the linear model between the two parameters for temperature lower than $15\,°C$ and the average of Q_F estimate for temperatures higher than $15\,°C$. This figure is available in colour online at www.interscience.wiley.com/ijoc
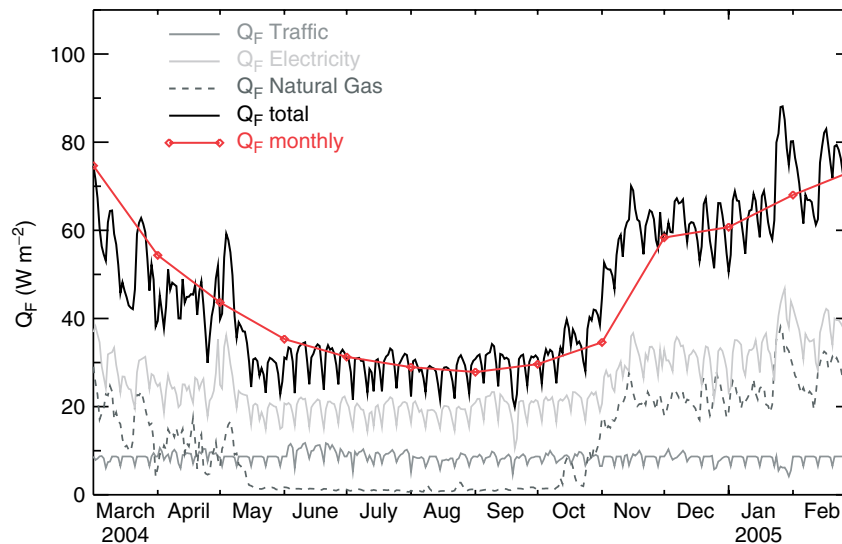
Figure 4. Evolution of mean daily Q_F from inventory according to the various sources. The black line represents the sum of the various terms, computed each day, whereas the diamonds are month averages. This figure is available in colour online at www.interscience.wiley.com/ijoc
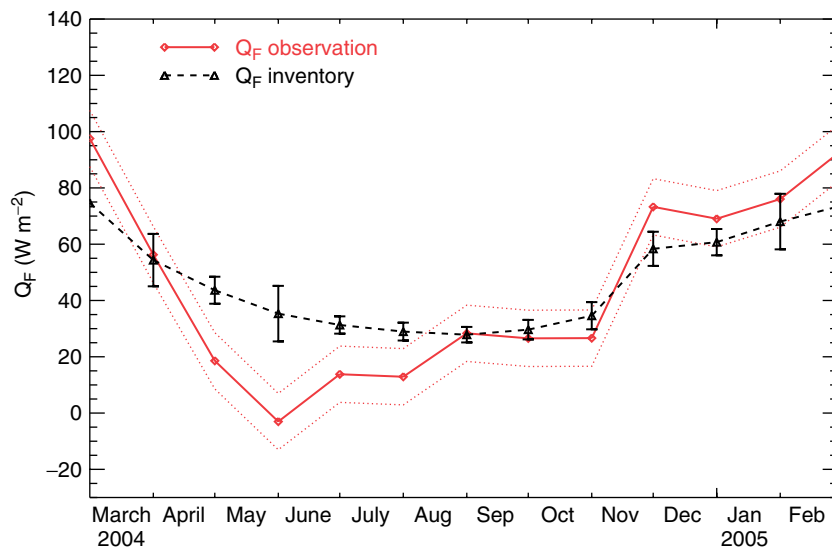

Figure 5. Comparison of monthly estimates of Q_F computed from measurements (solid line and diamonds, red in colour version) and from inventory (dashed line, triangles and black in colour version). For Q_F estimated from the micro-meteorological measurements, the two dotted lines represent ± 10 W m^{-2} following Offerle *et al.* (2005) recommendations. The bars for Q_F estimated from the inventory represent the variability inside the month. This figure is available in colour online at www.interscience.wiley.com/ijoc

2004 with a resolution of 100 m. The value during this period is the basal level (Q_F^b) which must be prescribed for modelling. In the centre of the city and in other areas with a dense building pad, the flux ranges between 5 and 25 W m^{-2}. This is quite comparable to what was observed in Łódź by Kłysik (1995), who found for the densest area of the city a mean summer Q_F of 14 W m^{-2}. In the suburban residential areas of Toulouse, it is lower than 5 W m^{-2}, whereas Kłysik (1995) proposes a value of 2 W m^{-2}. Over the agglomeration, the average is 7.7 W m^{-2}, which is comparable to what has been reported by Sailor and Lu (2004) for Salt Lake City (Utah) for this period of the year.

The traffic is the dominant term of the basal level. All the major roads of the network clearly appear on

Figure 6. Three categories of roads have a significant impact on Q_F:

- the roads connecting districts of Toulouse (two lanes);
- the major roads (four lanes or more);
- the motorway rounding the Toulouse district.

During summer, Q_{FT} could be expected to be lower than during the rest of the year because of vacations. Using the 21 permanent traffic counters, the traffic has been compared between summer (July and August) and the rest of the year. The difference has been found to be lower than 10% and is, therefore, neglected in this study. The description of the spatio-temporal variability presented in this section can be used to constrain
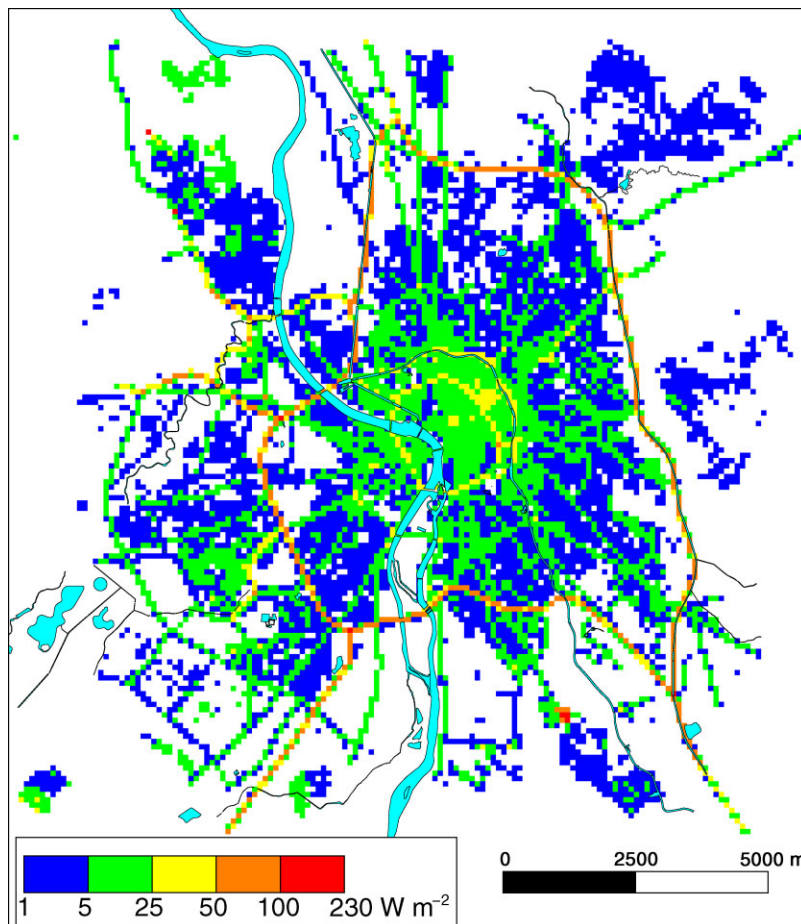
Figure 6. Spatial variation of Q_F over the agglomeration, averaged over June, July and August 2004. Q_F during this period represents the basal level. This figure is available in colour online at www.interscience.wiley.com/ijoc

numerical simulation at the agglomeration scale. To summarise, some typical values are gathered in Table VII to estimate the impact of a 100-m long road on a cell of 100 m × 100 m. Considering the mean annual values of Q_{FT}, the impact of the latent heat released by traffic (8%) is only significant on the busiest sections of the motorways and never exceeds 10 W m^{-2}.

Weekly and daily cycles of Q_F

Traffic. Regarding traffic, since the available data are in general the MANDVs, the Q_F cycles have been normalised by this value. The left graph on Figure 7 represents the weekly cycle. Saturdays and Sundays

Table VII. Typical Q_{FT} released by a 100-m road in a 100-m × 100 m cell.

		Traffic	Q_{FT} (W m^{-2})
Downtown roads	Vehicles per day	10 000	5.5
	Hourly traffic peak	700	9.2
Major roads	Vehicles per day	20 000	10.9
	Hourly traffic peak	1400	18.3
Motorway ring	Vehicles per day peak	100 000	54.5
	Vehicles per hour	7000	91.6

present differences with weekdays of nearly 25%. On the right panel of the figure, the daily cycle is represented for both weekdays and week-end and hourly values are expressed as a fraction of the daily traffic. These profiles are really close to what had been presented by Sailor and Lu (2004). In US cities and in Toulouse, the morning peak of traffic is short and accounts for about 7% of daily traffic. The evening peak extends on a longer period.

Electricity. A weekly profile for electricity (left panel of Figure 8) is found to be representative of the whole year without any seasonal distinction. This profile is close to the traffic weekly profile. A lower consumption is recorded on Saturdays and Sundays. The difference between weekdays and week-end is about 20%. The daily cycle (right panel of Figure 8) varies with the season as reported by Sailor and Lu (2004). During summer, there is an increase in consumption during the day, which follows human activities. During winter, there is also an increase during the day with peaks in the morning and in the evening. These peaks are associated to lighting. On the other hand, a peak during the night appears during summer and winter and is correlated to the lowering of electricity price. Applications such as water heating are often scheduled to start at this time. This peak is
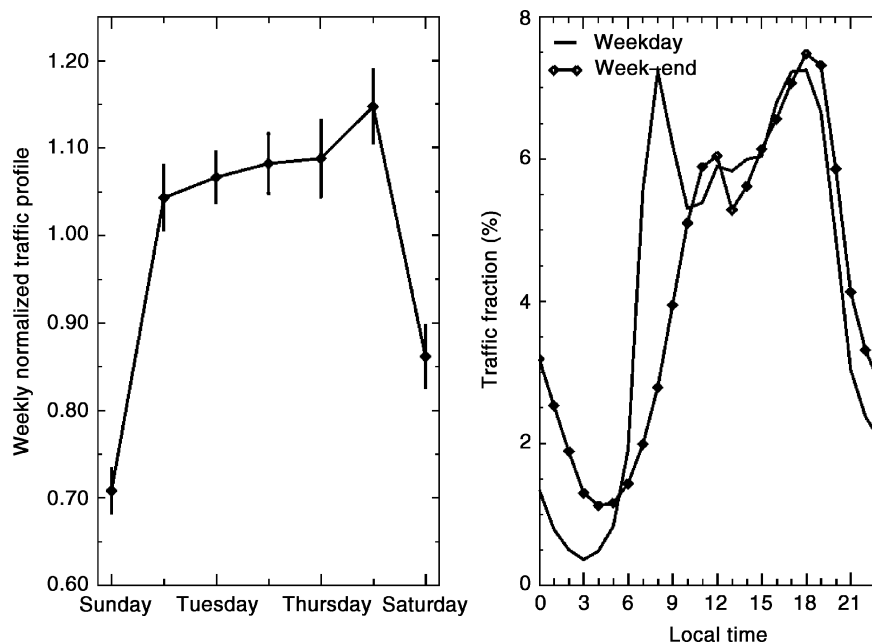
Figure 7. Weekly and daily normalised traffic profiles for weekday and week-end based on measurements of 21 points over Toulouse during the years 2003 and 2004.

certainly typical of France and cannot be seen in the profiles presented by Sailor and Lu (2004).

Gas. Only the gas daily consumptions were available. The annual cycle normalised by the weekly average is represented on the top panel of Figure 9. The week cycle is significant during summer but it vanishes during winter, even if we remove the effect of the daily mean temperature. The week cycle identified during the summer period has been computed (bottom panel of Figure 9) and is assumed to represent the basal level of consumption. In Toulouse, gas is mainly used for domestic heating and we assume that the gas cycle is representative of all other minor sources of energy that can be used for heating (domestic fuel, urban network, wood, coal).

Modelling framework of temporal variation. To conclude this section, we propose a set of equations that represents the temporal variation each sources of energy and that can be used for modelling purpose:

$$Q_{FT}(t) = Q_{FT}^y \times P_T^w(d) \times P_T^d(h) \qquad (7)$$

$$Q_{Fe}(t) = (Q_{Fe}^C(t) + Q_{Fe}^b) \times P_e^w(d) \times P_e^d(S, h) \quad (8)$$

$$Q_{Fhf}(t) = Q_{Fhf}^C(t) + Q_{Fhf}^b \times P_{hf}^w(d) \qquad (9)$$

Equation (7) describes the temporal evolution of heat released by traffic, for which the mean annual value (Q_{FT}^y) is modulated by the week cycle ($P_T^w(d)$) and the daily cycle ($P_T^d(h)$). Equation (8) expresses the temporal evolution of heat released by electricity. $Q_{Fe}^C(t)$ is the climatic contribution of Q_{Fe}, which is physically computed in models such as TEB and which mainly represents the heating of buildings. Q_{Fe}^b gathers the basal

flux. Both values are affected by the week cycle ($P_e^w(d)$) and the daily ($P_e^d(S, h)$) cycle, which varies with the season (variable S). Finally, Equation (9) represents the temporal variation of the heat released by the combustion of fossil fuels (used for building and water heating). As for gas, the climatic component ($Q_{Fhf}^C(t)$) is independent of the week cycle and responds to rapid variations (one day) of meteorological conditions. In the end, a basal state of consumption (Q_{Fhf}^b), modulated at least by a week cycle ($P_{hf}^w(d)$), have to be added to the climatic component.

Q_F during winter time

To represent the seasonal evolution of Q_F, a map over the agglomeration is presented for the winter period (Figure 10) with the same colour scale than the summer period (Figure 6). For the centre of Toulouse, Q_F can reach 100 W m^{-2} in the densest areas. In comparison, Kłysik (1995) estimated a value of 73 W m^{-2} for Łódź. In residential suburban areas, the values are generally between 5 and 25 W m^{-2}, while Kłysik (1995) recorded a mean value of 8 W m^{-2}. During winter time and in the dense urban areas, Q_F is dominated by heating demand. Over the agglomeration, the average is 17.3 W m^{-2}, which is comparable to what has been reported by Sailor and Lu (2004) for Los Angeles during the same period of the year.

CONCLUSIONS

The anthropogenic heat releases have been estimated for the agglomeration of Toulouse from February 2004 to March 2005. At the local scale over a dense urban area, SEB measurements have been conducted and a method is
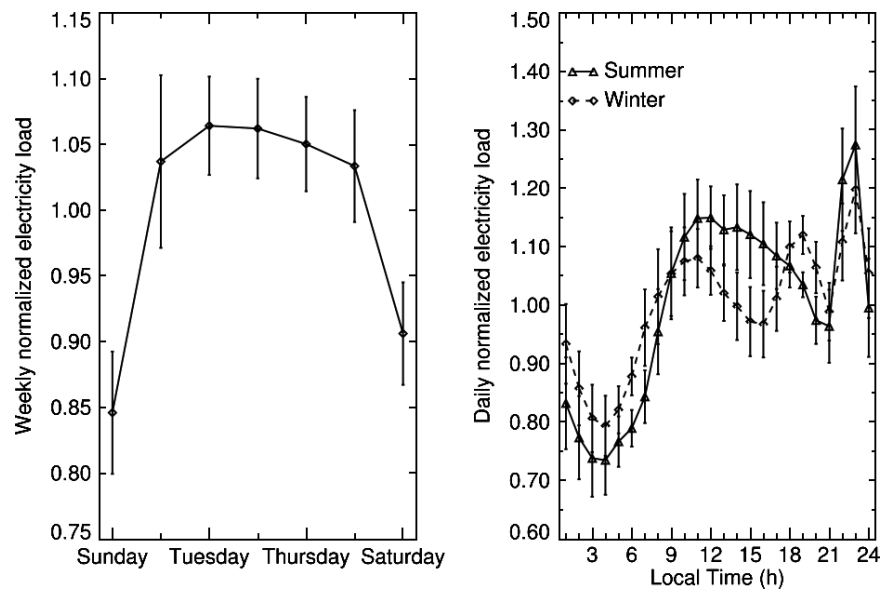
Figure 8. Weekly (left) and daily (right) normalised cycles of electricity power load during the field campaign.
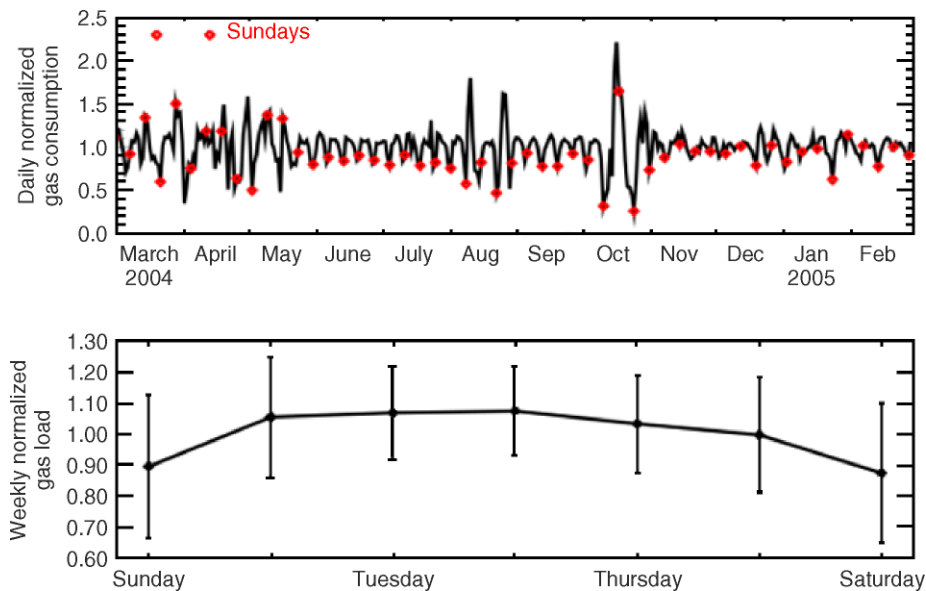

Figure 9. Annual (top) and weekly (bottom) normalised cycles of gas consumption during the field campaign. Weekly cycle is computed for the basal level of consumption (summer). This figure is available in colour online at www.interscience.wiley.com/ijoc

proposed to estimate Q_F from these observations. Values obtained from this method present a general in agreement with what was expected, i.e. Q_F exhibits a linear decrease with the mean daily air temperature (6.8 W m^{-2} K^{-1}), except when temperature is higher than 15 °C (warm season). In the latter case, Q_F varies around a mean value of 16 W m^{-2}. A part of the scatter observed around this mean value could result from uncertainties in the measurements of the sensible and latent heat fluxes.

At the agglomeration scale, an inventory of energy consumption was conducted for the period covered by the field campaign. Hourly cycles were available for traffic and electricity. For gas, data were available at a 1-day resolution. For other sources of energy (minor contribution), only annual statistical data were available.

The inventory was rasterized over the agglomeration with a resolution of 100 m × 100 m by combining the real time series of energy consumption with data on the land use and energy consumption for various housing types.

At the local scale (500 m) around the downtown measurements site, we compared the estimates of Q_F computed from the SEB observations and from the inventory. This point is an important innovation of the present study. For winter, the second half of spring and fall, both estimates agree and give values of Q_F around 70 W m^{-2}. It should be noted that this value exceeds that of the daily net radiation during the winter season. From the end of May to August, the estimates computed from the inventory are around 30 W m^{-2}, which is 15 W m^{-2} higher than the values computed
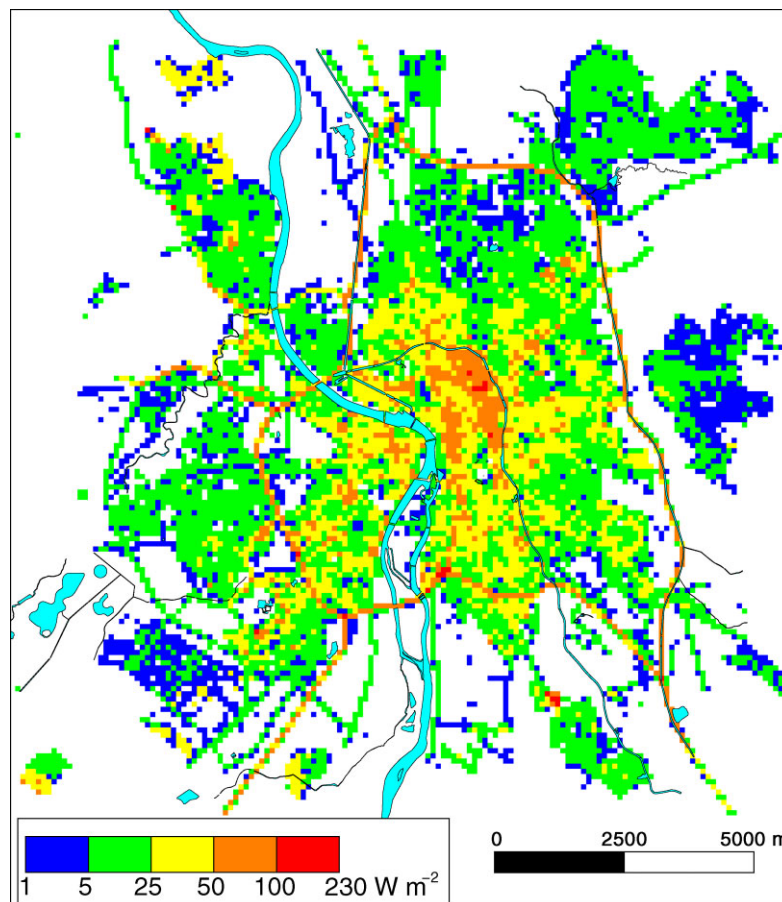
Figure 10. Spatial variation of Q_F over the agglomeration, averaged over December 2004, January and February 2005. This figure is available in colour online at www.interscience.wiley.com/ijoc

from the SEB measurements. A possible explanation of these low values of measured Q_F is the well-known underestimation of Q_H and Q_E with the eddy-covariance technique, particularly during the warm period when the term $Q_H + Q_E$ is at its highest level.

At the agglomeration scale, the basal level of energy consumption (summer period) varies between 25 W m^{-2} for the densest areas to values lower than 5 W m^{-2} for the residential suburban areas. In the areas crossed by major roads, the traffic constitutes the main source of Q_F. For the winter period, the densest areas of Toulouse experienced Q_F as high as 100 W m^{-2} whereas it laid between 5 and 25 W m^{-2} over the suburban areas.

Modelling studies over the agglomeration of Toulouse will benefit from this inventory. Mesoscale atmospheric models that have a resolution fine enough to describe large agglomerations such as Toulouse have to represent the anthropogenic heat releases in their surface-atmosphere exchange scheme. This term is either prescribed or (partially) computed by the model. The results presented in this paper can provide input parameters and validation data for these models.

REFERENCES

Arnfield AJ, Grimmond CSB. 1998. An urban energy budget model and its application to urban storage heat flux modeling. *Energy and Buildings* **27**: 61–68.

Christen A, Vogt R. 2004. Energy and radiation balance of a central European city. *International Journal of Climatology* **24**: 1395–1421.

Foken T. 2006. The energy balance closure problem: an overview. In *ILEAPS Specialist Workshop: Flux Measurements in Difficult Conditions*, Boulder, CO, 26–28 January.

Grimmond CSB. 1992. The suburban energy balance: methodological considerations and results for a mid-latitude west coast city under winter and spring conditions. *International Journal of Climatology* **12**: 481–497.

Grimmond CSB, Oke TR. 1999. Heat storage in urban areas: observations and evaluation of a simple model. *Journal of Applied Meteorology* **38**: 922–940.

Grimmond CSB, Cleugh HA, Oke TR. 1991. An objective urban heat storage model and its comparison with other schemes. *Atmospheric Environement* **25**: 311–326.

Guibet JC. 1997. *Carburants et moteurs*. Technip: Paris.

Hugrel C, Joumard R. 2004. Transport routier -parc, usage et émission des véhicules en France de 1970 à 2025. Technical Report Rapport LTE n°0420, INRETS. pp 129, in French.

Hugrel C, Joumard R. 2006. Directives et facteurs agrégés d'émission des véhicules routiers en france de 1970 à 2025. Technical Report 611, INRETS-LTE. pp 150, in French.

Ichinose T, Shimodozno K, Hanaki K. 1999. Impact of anthropogenic heat on urban climate in Tokyo. *Atmospheric Environment* **33**: 3897–3909.

Khan SM, Simpson RW. 2001. Effect of a heat island on the meteorology of a complex urban airshed. *Boundary-Layer Meteorology* **100**: 487–506.

Kikegawa Y, Genchi Y, Kondo H, Hanaki K. 2006. Impacts of city-block-scale countermeasures against urban heat-island phenomena upon a buildings energy-consumption for air-conditioning. *Applied Energy* **83**: 649–668.

Kimura F, Takahashi S. 1991. The effects of land-use and anthropogenic heating on the surface temperature in the Tokyo metropolitan area: a numerical experiment. *Atmospheric Environment* **25B**: 155–164.

Kłysik K. 1995. Spatial and seasonal distribution of anthropogenic heat emissions in Łódź, Poland. *Atmospheric Environment* **30**: 3397–3404.

Kohsiek W, Liebethal C, Foken T, Vogt R, Oncley SP, Bernhofer C, DeBruin HAR. 2007. The energy balance experiment EBEX-2000, part III: Radiometer comparison. *Boundary-Layer Meteorology* online first, DOI: 10.1007/s10546-006-9135-8, **123**: 55–75.

Lee X, Hu X. 2002. Forest-air fluxes of carbon, water and energy over non-flat terrain. *Boundary-Layer Meteorology* **103**: 277–301.

Lemonsu A, Grimmond CSB, Masson V. 2004. Modeling the surface energy balance of the core of an old mediterranean city: Marseille. *Journal of Applied Meteorology* **43**: 312–327.

Massera S. 2005. Exploitation d'une base de données urbaines en vue d'extraire des paramètres utiles aux modèles météorologiques. Technical report, Meteo France, in French. Available on request from the corresponding author.

Masson V. 2000. A physically-based scheme for the urban energy budget in atmospheric models. *Boundary-Layer Meteorology* **94**: 357–397.

Masson V, Pigeon G, Durand P, Gomes L, Salmond J, Lagouarde JP, Voogt JA, Oke TR, Lac C, Liousse C, Maro D. 2004. The Canopy and Aerosol Particles In TOulouse Urban Layer (CAPITOUL) experiments: first results. In AMS Editions, editor, *PROCEEDINGS of the Fifth Symposium on the Urban Environment*, Vancouver, Ca, 23–27 Aug.

Mauder M, Oncley SP, Vogt R, Weidinger T, Ribeiro L, Bernhofer C, Foken T, Kohsiek W, De Bruin HAR, Liu H. 2007. The energy balance experiment EBEX-2000. part II: inter-comparison of eddy covariance sensors and post-field data processing methods. *Boundary-Layer Meteorology online first*, **123**: 29–54, DOI: 10.1007/s10546-006-9139-4.

McMillen RT. 1988. An eddy correlation technique with extended applicability to non-simple terrain. *Boundary-Layer Meteorology* **43**: 231–245.

Offerle B, Grimmond CSB, Fortuniak K. 2005. Heat storage and anthropogenic heat flux in relation to the energy balance of a central European city centre. *International of Journal Climatology* **25**: 1405–1419.

Oke TR. 1982. The energetic basis of the urban heat island. *Quarterly Journal of the Royal Meteorological Society* **108**: 1–24.

Oke TR. 1987. *Boundary Layer Climates*. Methuen, London and New York, 435.

Oke TR. 1988. The urban energy balance. *Progress in Physical Geography* **12**: 471–508.

Oke TR. 2004. Initial guidance to obtain representative meteorological observations at urban sites. IOM report N° 81, WMO/TD N°1250. World Meteorological Organization, Geneva.

Oke TR. 2006. Towards better scientific communication in urban climate. *Theoretical and Applied Climatololgy* **84**: 179–190.

Oke TR, Cleugh HA. 1987. Urban heat storage derived as energy balance residuals. *Boundary-Layer Meteorology* **39**: 233–245.

Oke TR, Spronken-Smith RA, Jauregui E, Grimmond CSB. 1999. The energy balance of central Mexico City during the dry season. *Atmospheric Environment* **33**: 3919–3930.

Pigeon G, Augustin C, Legain D, Durand P, Masson V. 2004. Characteristics of the urban thermodynamic island and the energy balance on Toulouse (FRANCE) during winter and spring periods of the CAPITOUL experiment. In AMS Editions, editor, *PROCEEDINGS of the Fifth Symposium on the Urban Environment*, 23–27 Aug.

Pigeon G, Lemonsu A, Grimmond CSB, Durand P, Thouron O, Masson V. 2007. Divergence of turbulent fluxes in the surface layer: case of a coastal city. *Boundary-Layer Meteorology* **124**: 269–290.

Sailor DJ, Lu L. 2004. A top-down methodology for developing diurnal and sea-sonal anthropogenic heating profiles for urban areas. *Atmospheric Environment* **38**: 2737–2748.

Spronken-Smith RA, Kossmann M, Zawar-Reza P. 2005. Where does all the energy go? Surface energy partitioning in suburban Christchurch under stable wintertime conditions. *Theoretical and Applied Climatology* **84**: 137–149.

Wanner H, Filliger P. 1989. Orographical influence on urban climate. *Weather and Climate* **9**: 22–28.

Weber S. 2005. Comparison of in-situ measured ground heat fluxes within an heterogeneous urban ballast layer. *Theoretical and Applied Climatology* **83**: 169–179.

Wilson K, Goldstein A, Falge E, Aubinet M, Baldocchi D, Berbigier P, Bernhofer C, Ceulemans R, Dolman H, Field C, Grelle A, Ibrom A, Law BE, Kowalski A, Meyers T, Moncrieff J, Monson R, Oechel W, Tenhunen J, Valentini R, Verma S. 2002. Energy balance closure at FLUXNET sites. *Agricultural and Forest Meteorology* **113**: 223–243.